ARTICLES

Theoretical Investigation of Excited States of Oligothiophene Anions

Fahri Alkan and Ulrike Salzner*

Department of Chemistry, Bilkent University, 06800 Bilkent, Ankara, Turkey

Received: November 23, 2007; Revised Manuscript Received: April 10, 2008

Electron−hole symmetry upon p- and n-doping of conducting organic polymers is rationalized with Hückel theory by the presence of symmetrically located intragap states. Since density functional theory (DFT) predicts very different geometries and energy level diagrams for conjugated π-systems than semiempirical methods, it is an interesting question whether DFT confirms the existence of electron−hole symmetry predicted at the Hückel level. To answer this question, geometries of oligothiophene anions with 5−19 rings were optimized and their UV/vis spectra were calculated with time-dependent DFT. Although DFT does not produce symmetrically placed sub-band energy levels, spectra of cations and anions are almost identical. The similarity in transition energies and oscillator strengths of anions and cations can be explained by the fact that the single sub-band energy level of cations lies above the valence band by the same amount of energy as the single sub-band level of anions lies below the conduction band. This and the resemblance of the energy level spacings in valence bands of cations to those in conduction bands of anions give rise to peaks with equal energies and oscillator strengths.

Introduction

Doping experiments on conducting organic polymers (COPs) revealed that oxidation and reduction lead to bleaching of the $\pi-\pi^*$ transition of the neutral species and development of one or two sub-band transitions.[1–6] Interestingly, for polyacetylene (PA) the nature of the counterion and even the sign of the charge, positive or negative, make little difference.[7] Such behavior was rationalized with a midgap state[8] which leads to electron−hole symmetry as holes in the valence band and electrons in the conduction band have similar energies. For polymers with nondegenerate ground states such as polypyrrole and polythiophene (PT), two intragap states are predicted and electron−hole symmetry may or may not be present, depending on the strength of interaction of the heteroatom with the backbone.[9] At the Hückel level, the deviation from electron−hole symmetry was shown to be very small for PT.[9] Experimentally, PT is usually investigated in the p-doped (oxidized) state[4–6,10]

since it can be n-doped (reduced) only with difficulty.[11,12] Thus experimental data on n-doping of PT are sparse.

Doping can be monitored with in situ UV/vis spectroscopy. During doping the interband transition of the neutral polymer disappears and two sub-band transitions emerge.[6] Spectral changes upon p-doping of PT were rationalized with an energy level diagram as shown in Scheme 1.[6] $h\nu1$ and $h\nu2$ are the energies of the sub-band absorptions (0.60−0.64 and 1.4−1.45 eV) of the p-doped polymer, which add up to the band gap of neutral PT (onset of absorption at 2.1 eV).[6] Both levels were assumed to be unoccupied (bipolaron formation) because three transitions were expected if one level were occupied (polaron formation).[13–17] That the two intragap levels are placed symmetrically was rationalized by a small interaction of the sulfur atom with the conjugated backbone.[6] For n-doped PT, both intragap levels are occupied. Excitation then occurs between the intragap states and the conduction band. As in the case of PA, similar UV spectra are expected for p-doped and n-doped PT. UV/vis spectra recorded during electrochemical n-doping of PT[18] seem to show trends similar to those recorded during

* To whom correspondence should be addressed. E-mail: salzner@fen.bilkent.edu.tr.

SCHEME 1
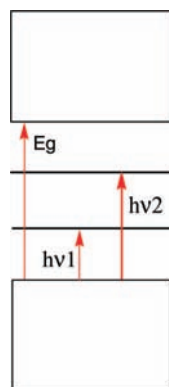
p-doping.[6] However, the bands are very broad. Electron−hole symmetry was confirmed experimentally for didodecylsexithiophene, which forms stable mono- and dications and anions.[19]

In contrast to the predictions based on the polaron−bipolaron model (Scheme 1),[13–17] experimental doping studies of oligothiophenes (OTs) in solution[20–35] showed that monocations (polarons) are associated with two sub-band transitions, while dications (bipolarons) give rise to only one sub-band feature. This was confirmed with theoretical investigations at various semiempirical[36–39] and ab initio levels,[34,40] and with density functional theory (DFT).[41–43] DFT orbital energy plots do not show symmetrically positioned energy levels in the gap, and the electronic transitions are only in some cases dominated by a single electron configuration.[43] Since the polaron−bipolaron model and diagrams like that in Scheme 1 are therefore confirmed neither by experiment nor by theory, the question arises of how electron−hole symmetry can be rationalized in PT. To compare p-doping and n-doping in PT, we performed DFT and time-dependent DFT calculations on radical anions of oligothiophenes (OTs) at the same level of theory that was previously used for radical cations and analyzed the spectra.[43]

Methods

Anions of thiophene oligomers with up to 19 rings (nT^-, n = number of rings) were optimized with density functional theory employing the B3P86[44,45] functional with 30% of Hartree−Fock exchange[46] and Stevens−Basch−Krauss pseudopotentials[47,48] with polarized split valence basis sets (CEP-31G* keyword in Gaussian 03[49]). All species were kept planar and have C_{2h} (even number of rings) and C_{2v} (odd number of rings) symmetries. Vertical excited states were calculated by using time-dependent DFT[50–53] with the B3P86-30% functional. Results of these calculations are compared with excitation energies of monocations of thiophene oligomers obtained at the same level of theory.[43] All calculations were done with Gaussian 03, revision D02.[49]

The B3P86-30%/CEP-31G* level of theory was tested and was shown to be reliable for oligothiophene radical cations.[43] However, anions are much more difficult to treat theoretically than cations. Especially small systems are challenging since they require proper accounting of electron correlation and large basis sets because of their diffuse charge clouds.[54] DFT was shown to be able to include enough correlation for anions,[55,56] and both correlation and basis set problems are much less crucial for large systems as the extra electron has more space and does not increase the size of the charge cloud significantly. Thus DFT with moderate basis sets was proven to be adequate to calculate properties of n-doped conjugated oligomers.[57] The same reasoning applies to excited-state calculations, which are much more complicated for small than for large systems.[58] Nonetheless, excited-state calculations of anions might require diffuse functions. To ensure that the CEP-31G* without diffuse functions is adequate, $9T^-$ was optimized and its excited states were calculated with the 6-31+G* basis set. As with CEP-31G* three excited states below 2.50 eV with oscillator strength larger than 0.3 were found. The values with the 6-31+G* basis set are 0.61 eV ($f = 1.12$), 1.48 eV ($f = 1.48$), and 2.50 eV ($f = 0.27$). Comparison with CEP-31G* results in Table 1 shows that the largest differences with and without diffuse functions are that the second peak has a 0.12 eV larger excitation energy with 6-31+G* and a 0.06 smaller oscillator strength. Therefore, diffuse functions, which cause convergence problems and increase the computational time, are not necessary and were not employed further.

Counterions and solvent have only a small effect on excitation energies of small to medium-sized thiophene cations. Therefore, gas phase calculations predict spectra very similar to those of calculations in the presence of counterions and solvent. To test whether the same is true for anions, $5T^-$ was optimized with the polarized continuum method (PCM)[59] in the presence of CH_2Cl_2 as solvent, with a sodium counterion in the gas phase, and with a sodium counterion in the presence of CH_2Cl_2. In contrast to negatively charged counterions that prefer to lie in the plane of the backbone, sodium prefers to sit above a ring. This is in agreement with electrostatics since carbon atoms carry negative partial charges and hydrogen atoms are charged positively. Thus, positive counterions such as sodium prefer to be close to the carbon atoms and negative ones such as Cl_3^- approach the hydrogen atoms. For cations, including solvent alone leads to a small red shift (∼0.1 eV) of the excitation energies, and the presence of a sodium counterion causes a small blue shift. Effects due to the simultaneous presence of counterion and solvent cancel partially. Stick spectra showing the gas phase and the solution spectrum in the presence of a counterion for $5T^-$ are presented in Figure 1. Only the first excitation energy is increased by 0.18 eV; the second one is unchanged. Since the effects are very small, and since we are interested here mainly in a comparison of theoretical results for anions and cations, gas phase calculations will be employed in the following.

Electron configurations contributing to the excited states are designated with a slightly modified Pariser[60] notation as shown in Scheme 2. π-Orbitals of neutral oligomers are numbered starting from the frontier orbitals with 1 for occupied and 1′ for unoccupied orbitals. Numbers increase with moving to lower and higher lying levels. The same numbering is used for anions, where the 1′ level contains now one electron. The lowest-lying excited states of anions arise from 1′−2′ and 1−1′ electronic transitions, which may mix. Higher energy excited states of long oligomer anions involve additional electronic transitions between higher- and lower-lying orbitals.

Results

Geometries. Electron affinities of 5T−19T were calculated with the ΔSCF method as energy differences between neutral species and anion. The electron affinities range from 1.82 eV for 5T to 2.57 eV for 19T. These gas phase estimates appear to be quite reasonable as they converge to a slightly smaller electron affinity value than the 3.0 eV estimated for polythiophene films by subtracting the experimental band gap (2.0 eV)[61] from the experimental ionization potential (5.0 eV).[62]

Figure 2 compares changes in the bond length upon n- and p-doping compared to neutral 19T. Bond length changes for anion and cation[43] are quite similar. In both cases the defect is delocalized and tends to separate into two regions. In both cases the changes are too small to invert the single−double bond

Excited States of Oligothiophene Anions

J. Phys. Chem. A, Vol. 112, No. 27, 2008 **6055**

TABLE 1: Energies and Oscillator Strengths (in Parentheses) of the Three Transitions for 5T−19T Anions and Cations

cations	E1	E2	E3	anions	E1	E2	E3
5T$^+$	1.12 (0.33)	1.86 (1.53)		5T$^-$	1.02 (0.35)	1.80 (1.32)	
6T$^+$	0.96 (0.53)	1.68 (1.70)		6T$^-$	0.89 (0.52)	1.64 (1.50)	
6T$^+$, expt^a	0.87	1.60			0.72	1.58	
8T$^+$	0.74 (1.00)	1.45 (1.75)	2.56 (0.16)	8T$^-$	0.69 (0.91)	1.43 (1.65)	
9T$^+$	0.65 (1.23)	1.37 (1.67)	2.42 (0.38)	9T$^-$	0.61 (1.11)	1.36 (1.54)	2.44 (0.30)
12T$^+$	0.46 (1.76)	1.21 (1.21)	2.14 (1.38)	12T$^-$	0.44 (1.57)	1.22 (1.27)	2.15 (1.11)
13T$^+$	0.41 (1.86)	1.17 (1.07)	2.08 (1.90)	13T$^-$	0.40 (1.67)	1.19 (1.14)	2.10 (1.56)
16T$^+$	0.31 (1.99)	1.09 (0.71)	2.00 (3.54)	16T$^-$	0.30 (1.81)	1.11 (0.82)	2.01 (3.24)
19T$^+$	0.24 (1.99)	1.05 (0.50)	1.95 (5.12)	19T$^-$	0.24 (1.83)	1.07 (0.60)	1.96 (4.82)

^{a} Experimental data are taken from ref 19 obtained on didodecylsexithiophene in CH_2Cl_2 with $FeCl_4^-$ as counterion for oxidation and in THF with K as counterion for reduction.
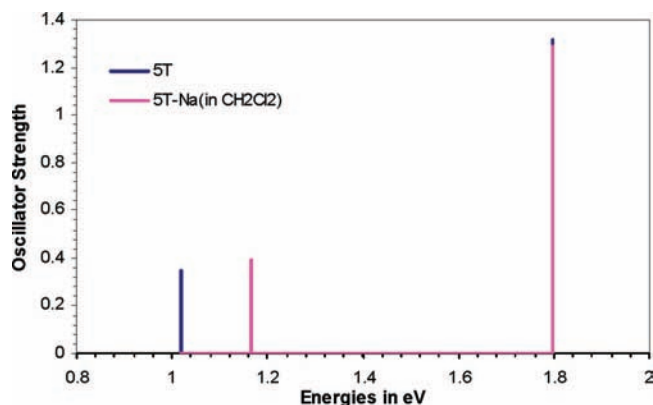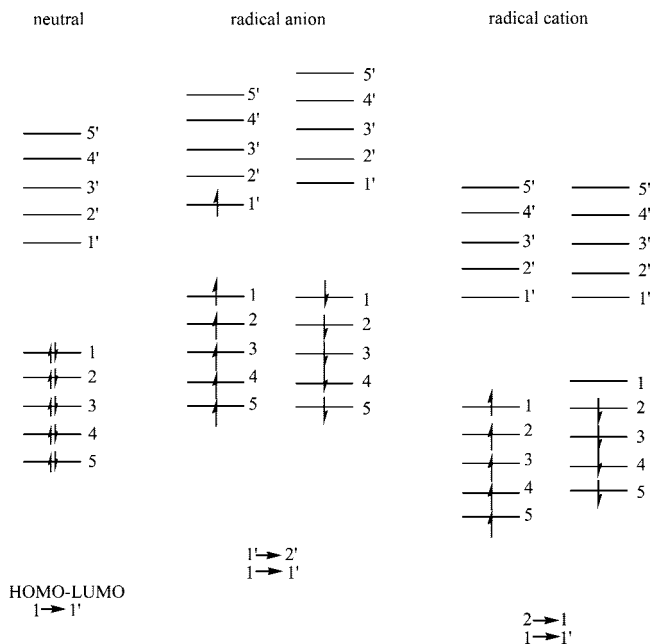

Figure 1. Effect of a counterion (Na$^+$) and solvent (CH_2Cl_2) on excitation energies of 5T$^-$.

SCHEME 2

Figure 2. C−C bond length changes of 19T anion (pink squares) and cation (blue diamonds) compared to neutral 19T.

Figure 3. Bond length changes in 13T$^-$ and 13T-Na compared to neutral 13T.

length pattern. Therefore, there is no transition to a quinoid structure in the absence of counterions for long oligomers.

Figure 3 shows bond length changes in 13T$^-$ and 13T-Na compared to neutral 13T. The presence of the counterion localizes the defect and increases the geometry distortion at the center of the chain where the sodium ion is located. The central rings are now quinoid. The first 12 carbon−carbon bond distances in the ion pair are unchanged compared to a neutral thiophene chain. Thus three rings on both sides are unaffected and the defect size amounts to seven thiophene rings. Therefore, the anionic defect is localized more strongly in the presence of
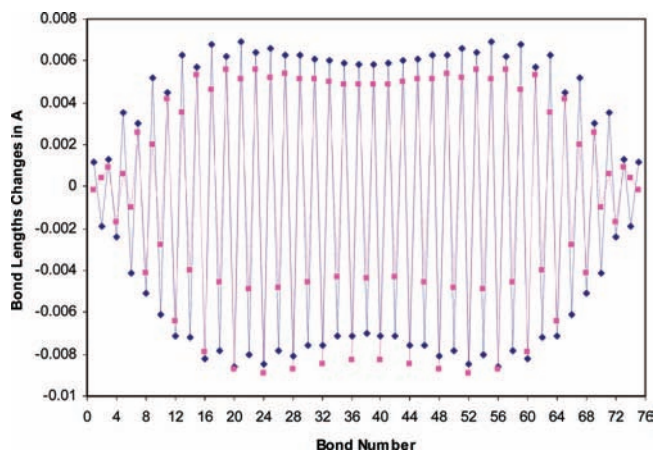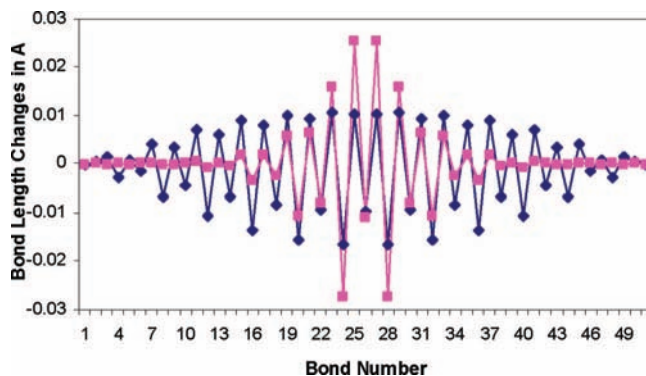
a Na counterion than the cationic defect in the presence of Cl$_3$, which spreads over 11 thiophene rings.[43] To assess the energetic effect of the geometry distortion, the counterion was removed from the ion pair and a single point energy calculation was performed on bare anion having the geometry with the localized defect. The energy of the anion in this nonequilibrium structure is 1.39 kcal/mol higher than that of the fully optimized anion with a delocalized defect. This shows that geometries of thiophene anions are very flexible and can adjust easily to the presence and location of counterions.

Excitation Energies. Excitation energies for 5T$^-$ through 19T$^-$ are listed and compared with those of the corresponding cations in Table 1. Stick spectra for 5T$^-$ through 8T$^-$ are plotted in Figure 4 and for 9T$^-$ through 19T$^-$ in Figure 5. All excitation energies with the exception of E3 for 9T$^-$ are smaller than the electron affinity of corresponding neutral form. Thus all excited states with the exception of E3 for 9T$^-$ are bound states and are stable with respect to electron loss, even in the gas phase.
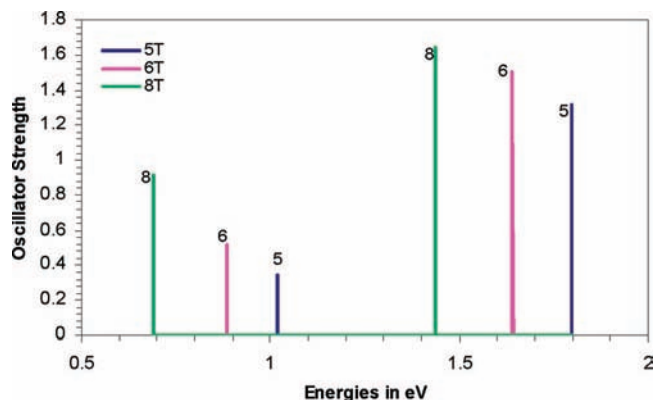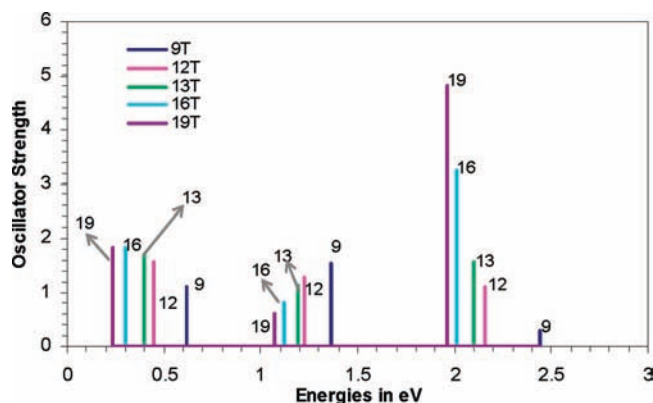
Figure 4. Stick spectra for 5T, 6T, and 8T anions.

Figure 5. Stick spectra for 9T, 12T, 13T, 16T, and 19T anions.

Figure 6. Excitation energy vs chain length of the three sub-band absorptions of 5T–19T anions.

Figure 7. Oscillator strength vs chain length of the three sub-band absorptions of 5T–19T anions.

$5T^-$ and $6T^-$ exhibit two sub-band transitions. The first peak arises from a $1'-2'$ transition (compare Scheme 2); the second is dominated by a $1-1'$ transition. Both excitations decrease in energy with increasing chain length for all species, and increase in oscillator strength up to $8T^-$. For $8T^-$ a third weak feature is predicted and the second and third absorptions arise from linear combination of $1-1'$ and $2-1'$ transitions with opposite signs.

Starting with $9T^-$, the third excitation has significant oscillator strength and the intensity of the second transition decreases with chain length. For $16T^-$ and $19T^-$, the third transition is the dominant peak. The inverse relationship of oscillator strengths of the second and third absorption peaks is caused by the fact that both transitions arise from the same electronic configurations, $1-1'$ and $2-1'$, with the latter, higher energy one gaining importance with increasing chain length.

The dependence of absorption energies and oscillator strength on chain lengths is summarized in Figures 6 and 7. It is seen that the three peaks of similar oscillator strength of $12 T^-$ and $13T^-$ are due to crossing of the oscillator strength of E3 with those of E1 and E2 on its way to becoming the dominant peak. Similarly to cations, spectral changes should occur when conjugation lengths reach large values.

Discussion

Geometry changes upon n-doping in oligomers of conducting organic polymers have been examined at various theoretical levels in the absence[9,63–65] and in the presence[66–71] of counterions. The main focus of these studies was to establish the defect size, charge distribution, and relative stability of polaron and bipolaron. While semiempirical methods predict smaller defect sizes for anions than for cations,[63] ab initio calculations find almost indistinguishable geometries for anions and cations.[65] Singly charged ions of thiophene oligomers are radicals with
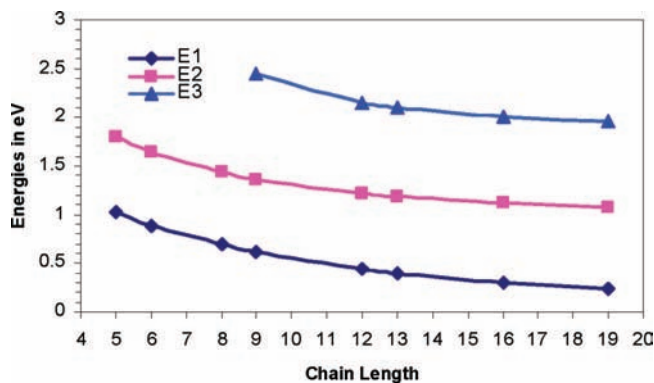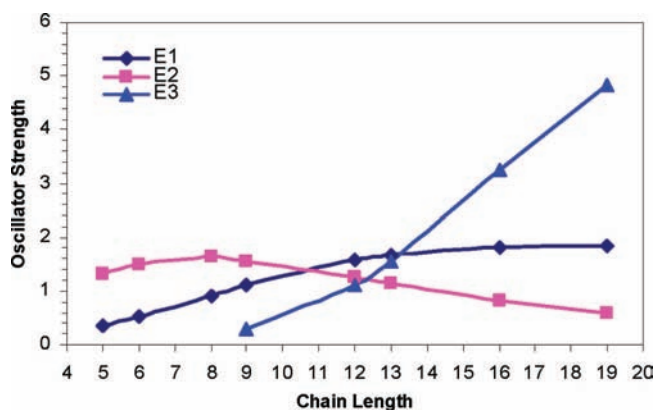
doublet ground states. Therefore, Hartree–Fock (HF), post-HF, and semiempirical methods based on HF theory are plagued by spin contamination, especially for long oligomers. For this reason comparisons of cationic and anionic defect sizes were done mainly on dications and dianions employing closed-shell calculations. These calculations cannot give final answers, as it emerged more recently that bipolarons are intrinsically unstable with respect to dissociation into polaron pairs.[43,72–75]

The problem with spin contamination can be circumvented for polyenes by using odd-numbered chains and examining spin-free cations and anions.[64] We employed the same trick recently to establish that the B3P86-30% functional produces geometries in close agreement with MP2 for odd-numbered polyene cations.[72] Thus B3P86-30%, in contrast to pure DFT,[72] does not overestimate defect sizes in COPs. We then showed that while there is severe spin contamination for even-numbered polyene radical cations with B3P86-30%, there is very little spin contamination for thiophene radical cations.[43] The same holds for the anions investigated here. The highest expectation value for the spin operator, we observe, is 0.82 for $8T^-$. Therefore, the B3P86-30% geometries are expected to be accurate and reliable. As shown in Figure 2, B3P86-30% predicts very similar geometries for cations and anions. In contrast to HF-based methods, however, the defect tends to spread over the whole chain. As shown in Figure 3, the defect localizes in the presence of a counterion. The strong geometry change is associated with a small energy difference (1.39 kcal/mol for $13T^-$) so that potential energy surfaces of charged thiophene oligomers are very flat and the systems are extremely flexible, adjusting their structures according to the presence and position of counterions.

To our knowledge, theoretical spectra of oligothiophene anions have never been reported. In contrast, excitation energies
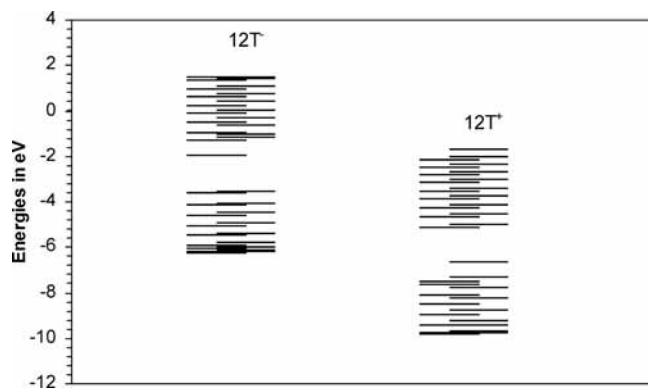
Excited States of Oligothiophene Anions

J. Phys. Chem. A, Vol. 112, No. 27, 2008 **6057**

Figure 8. Orbital energies of $12T^-$ (left) and $12T^+$ (right).

Figure 9. Electronic transitions contributing to the three peaks in the UV spectra of $12T^-$.

Figure 10. Electronic transitions contributing to the three peaks in the UV spectra of $12T^+$.

were predicted based on band structure calculations, using energy level differences directly as excitation energies and comparing theoretical results for n-doped polymers directly with experimental results on p-doped polythiophene.[66] As computers have improved dramatically in recent years, longer oligomers can be used now, structures can be fully optimized, and excitation energies can be calculated explicitly with reliable methods. UV-spectroscopic data[11,12] for n-doping of PT are not well resolved. However, absorption energies of didodecyl-sexithiophene cations and anions are available.[19] These data are included in Table 1. TDB3P86-30% excitation energies are between 0.06 and 0.17 eV higher than the experimental values. Compared to cations, anions absorb at slightly lower energy, by up to 0.15 eV (experimental) and 0.09 eV (TDB3P86-30%). This is an excellent agreement between theory and experiment which rivals the accuracy of the best ab initio methods for small molecules. Therefore, TDB3P86-30% is confirmed to be accurate enough to predict and analyze spectral properties of charged systems.

Based on energy diagrams like the one shown in Scheme 1, the polaron model, developed applying the Su−Schrieffer−Heeger (SSH) Hamiltonian,[13,76] predicts electron−hole symmetry. Thus UV spectra of p-doped and n-doped conducting polymers are expected to be similar. The symmetric spacing of the intragap states at the SSH level results from the fact that electronic interactions are not considered explicitly, which means that the number of electrons in those states does not alter the positions of the intragap levels. Applying density functional theory, the energies of the levels change considerably as electrons are added to the system. Orbital energy plots for $12T^+$ and $12T^-$ are compared in Figure 8.

Upon p-and n-doping, only one level appears in the gap. This DFT picture differs therefore from the energy level distribution according to the polaron model (Scheme 1) where two intragap levels are predicted. For the anion, an electron is added to the conduction band and the singly occupied level moves down in energy. For the cation, one electron is removed from the valence band and the singly occupied level moves up in energy. What is similar to Scheme 1 is that the energy difference of the anion level from the conduction band is almost identical to the energy difference of the cation level from the valence band (0.62 eV for the anion and 0.60 eV for the cation). The energy level diagrams of the anion and the cation look therefore like horizontal mirror images of each other. The calculated transitions between these energy levels are visualized in Figure 9 for $12T^-$ and in Figure 10 for $12T^+$.

There is a striking resemblance in the number of peaks, excitation energies, oscillator strengths, contributing electronic configurations, and coefficients of these configurations for the cation and the anion. The lowest energy peak is dominated by
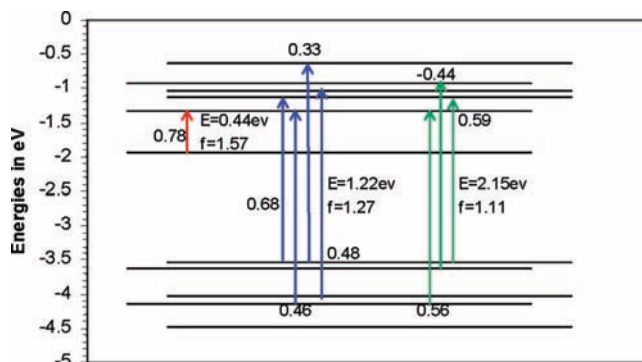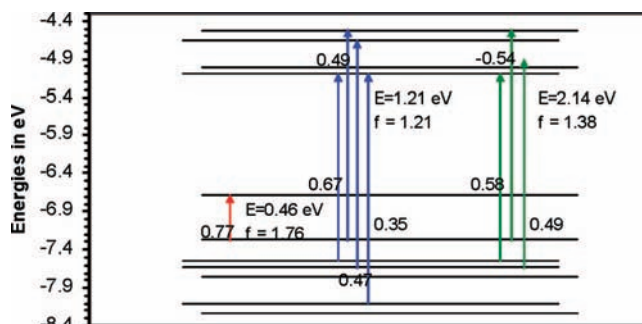
a single electron configuration, arising from the 2−1 transition (compare Scheme 2) for the cation and the 1′−2′ transition for the anion. Since there is little configuration interaction (CI), the identical excitation energies are due to the similar energy differences between the singly occupied molecular orbital (SOMO) and the occupied orbitals for the cation and between the SOMO and the unoccupied levels for the anion. The second and third excitation peaks are multiconfigurational. Nonetheless, excitation energies and oscillator strengths are very similar for the cation and the anion. Figures 9 and 10 show that the mirror-image symmetry of energy levels holds also for higher- and lower-lying energy levels and that the individual electronic transitions contributing to the excitation peaks have similar energy differences and CI coefficients. Excitation energies and oscillator strengths summarized in Table 1 for 5T−19T anions and cations show the same agreement between excitation energies and oscillator strengths for anions and cations at all chain lengths. Thus, although the energy level diagram at the DFT level of theory differs from that obtained with SSH, the hole−electron symmetry between anions and cations is confirmed with DFT.

Conclusions

Time-dependent density functional theory at the B3P86-30%/CEP-31G* level predicts excitation energies for oligothiophene anions in close agreement with experiment despite the relatively small basis set employed. In the absence of counterions, anionic defects in thiophene oligomers are delocalized. Nonetheless, sub-band transitions that agree with experiments are predicted. Thus sub-band transitions in ions are not linked to defect localization. Geometries of anions are very similar to those of cations. The presence of a counterion leads to stronger defect localization in anions than in cations. The extremely small energy difference between fully optimized $13T^-$ and $13T^-$ with the structure of 13T-Na shows that structures of anions, like those of cations, are very flexible.

6058 *J. Phys. Chem. A, Vol. 112, No. 27, 2008*

Alkan and Salzner

Oligothiophene anions and cations are predicted to have virtually identical UV spectra. There is therefore almost perfect electron−hole symmetry. Short oligothiophene anions give rise to two sub-band transitions; oligomers with more than eight rings exhibit three peaks. Since the third peak appears only at long chain length, it depends strongly on defect localization and therefore on the absence or presence of a counterion.

References and Notes

(1) Chiang, C. K.; Gau, S. C.; Fincher, C. R.; Park, Y. W.; MacDiarmid, A. G.; Heeger, A. J. *Appl. Phys. Lett.* **1978**, *33*, 18.

(2) Fincher, C. R., Jr.; Peebles, D. L.; Heeger, A. J.; Druy, M. A.; Matsamura, Y.; MacDiarmid, A. G.; Shirakawa, H.; Ikeda, S. *Solid State Commun.* **1978**, *27*, 489.

(3) Salaneck, W. R.; Thomas, H. R.; Duke, C. B.; Paton, A.; Plummer, E. W.; Heeger, A. J.; MacDiarmid, A. G. *J. Chem. Phys.* **1979**, *71*, 2044.

(4) Kaneto, K.; Yoshino, K.; Inuishi, Y. *Solid State Commun.* **1983**, *46*, 389.

(5) Kaneto, K.; Kohno, Y.; Yoshino, K. *Solid State Commun.* **1984**, *51*, 267.

(6) Chung, T.-C.; Kaufman, J. H.; Heeger, A. J.; Wudl, F. *Phys. Rev. B* **1984**, *30*, 702.

(7) Fincher, C. R., Jr.; Ozaki, M.; Heeger, A. J.; MacDiarmid, A. G. *Phys. Rev. B* **1979**, *19*, 4140.

(8) Fesser, K.; Bishop, A. R.; Campbell, D. K. *Phys. Rev. B* **1983**, *27*, 4804.

(9) Bertho, D.; Jouanin, C. *Phys. Rev. B* **1987**, *35*, 626.

(10) Tourillon, G.; Garnier, F. *J. Phys. Chem.* **1983**, *87*, 2289.

(11) Mastragostino, M.; Soddu, L. *Electrochim. Acta* **1990**, *35*, 463.

(12) Aizawa, M.; Watanabe, S.; Shinohara, H.; Shirakawa, H. *J. Chem. Soc., Chem. Commun.* **1985**, 264.

(13) Su, W. P.; Schrieffer, J. R.; Heeger, A. J. *Phys. Rev. B* **1980**, *22*, 2099.

(14) Brédas, J. L.; Scott, J. C.; Yakushi, K.; Street, G. B. *Phys. Rev. B* **1984**, *30*, 1023.

(15) Brédas, J. L.; Street, G. B. *Acc. Chem. Res.* **1985**, *18*, 309.

(16) Brédas, J. L.; Wudl, F.; Heeger, A. J. *Solid State Commun.* **1987**, *63*, 577.

(17) Heeger, A. J.; Kivelson, S.; Schrieffer, J. R.; Su, W.-P. *Rev. Mod. Phys.* **1988**, *60*, 781.

(18) Aizawa, M.; Shinohara, H.; Yamada, T.; Akagi, K.; Shirakawa, H. *Synth. Met.* **1987**, *18*, 711.

(19) Bäuerle, P.; Segelbacher, U.; Gaudl, K.-U.; Huttenlocher, D.; Mehring, M. *Angew. Chem., Int. Ed. Engl.* **1993**, *32*, 76.

(20) Evans, C. H.; Scaiano, J. C. *J. Am. Chem. Soc.* **1990**, *112*, 2694.

(21) Fichou, D.; Xu, B.; Horowitz, G.; Garnier, F. *Synth. Met.* **1991**, *41*, 463.

(22) Caspar, J. V.; Ramamurthy, V.; Corbin, D. R. *J. Am. Chem. Soc.* **1991**, *113*, 600.

(23) Zinger, B.; Mann, K. R.; Hill, M. G.; Miller, L. L. *Chem. Mater.* **1992**, *4*, 1113.

(24) Hill, M. G.; Penneau, J.-F.; Zinger, B.; Mann, K. R.; Miller, L. L. *Chem. Mater.* **1992**, *4*, 1106.

(25) Hill, M. G.; Mann, K. R.; Miller, L. L.; Penneau, J.-F. *J. Am. Chem. Soc.* **1992**, *114*, 2728.

(26) Bäuerle, P.; Segelbacher, U.; Maier, A.; Mehring, M. *J. Am. Chem. Soc.* **1993**, *115*, 10217.

(27) Wintgens, V.; Valat, P.; Garnier, F. *J. Phys. Chem.* **1994**, *98*, 228.

(28) Furukawa, Y. *Synth. Met.* **1995**, *69*, 629.

(29) Yu, Y.; Gunic, E.; Zinger, B.; Miller, L. L. *J. Am. Chem. Soc.* **1996**, *118*, 1013.

(30) Sato, M.; Hiroi, M. *Polymer* **1996**, *37*, 1685.

(31) Miller, L. L.; Mann, K. R. *Acc. Chem. Res.* **1996**, *29*, 417.

(32) Graf, D. D.; Duan, R. G.; Campbell, J. P.; Miller, L. L.; Mann, K. R. *J. Am. Chem. Soc.* **1997**, *119*, 5888.

(33) van Haare, J. A. E. H.; Havinga, E. E.; van Dongen, J. L. J.; Janssen, R. A. J.; Cornil, J.; Brédas, J. L. *Chem.−Eur. J.* **1998**, *4*, 1509.

(34) Keszthelyi, T.; Grage, M. M.-L.; Offersgard, J. F.; Wilbrandt, R.; Svendsen, C.; Sonnich Mortensen, O.; Pedersen, J. K.; Jensen, H. J. A. *J. Phys. Chem. A* **2000**, *104*, 2808.

(35) Nakanishi, H.; Sumi, N.; Ueno, S.; Takimiya, K.; Aso, Y.; Otsubo, T.; Komaguchi, K.; Shiotani, M.; Ohta, N. *Synth. Met.* **2001**, *119*, 413.

(36) Cornil, J.; Beljonne, D.; Brédas, J. L. *J. Chem. Phys.* **1995**, *103*, 842.

(37) Cornil, J.; Beljonne, D.; Brédas, J. L. *J. Chem. Phys.* **1995**, *103*, 834.

(38) Ye, A.; Shuai, Z.; Beljonne, D.; Brédas, J. L. *Synth. Met.* **2003**, *137*, 1077.

(39) Ye, A.; Shuai, Z.; Kwon, O.; Brédas, J. L.; Beljonne, D. *J. Chem. Phys.* **2004**, *121*, 5567.

(40) Rubio, M.; Ortí, E.; Pou-Amerigo, R.; Merchán, M. *J. Phys. Chem. A* **2001**, *105*, 9788.

(41) Grozema, F. C.; Candeias, L. P.; Swart, M.; van Duijnen, P. T.; Wildeman, J.; Hadziioanou, G.; Siebbeles, L. D. A.; Warman, J. M. *J. Chem. Phys.* **2002**, *117*, 11366.

(42) Gao, Y.; Liu, C.-G.; Jiang, Y.-S. *J. Phys. Chem. A* **2002**, *106*, 5380.

(43) Salzner, U. *J. Chem. Theor. Comput.* **2007**, *3*, 1143.

(44) Becke, A. D. *J. Chem. Phys.* **1993**, *98*, 5648.

(45) Perdew, J. P. *Phys. Rev. B* **1986**, *33*, 8822.

(46) Salzner, U.; Pickup, P. G.; Poirier, R. A.; Lagowski, J. B. *J. Phys. Chem. A* **1998**, *102*, 2572.

(47) Stevens, W.; Basch, H.; Krauss, J. *J. Chem. Phys.* **1984**, *81*, 6026.

(48) Stevens, W. J.; Krauss, M.; Basch, H.; Jasien, P. G. *Can. J. Chem.* **1992**, *70*, 612.

(49) Frisch, M. J.; Trucks, G. W.; Schlegel, H. B.; Scuseria, G. E.; Robb, M. A.; Cheeseman, J. R.; Montgomery, J. A., Jr.; Vreven, T.; Kudin, K. N.; Burant, J. C.; Millam, J. M.; Iyengar, S. S.; Tomasi, J.; Barone, V.; Mennucci, B.; Cossi, M.; Scalmani, G.; Rega, N.; Petersson, G. A.; Nakatsuji, H.; Hada, M.; Ehara, M.; Toyota, K.; Fukuda, R.; Hasegawa, J.; Ishida, M.; Nakajima, T.; Honda, Y.; Kitao, O.; Nakai, H.; Klene, M.; Li, X.; Knox, J. E.; Hratchian, H. P.; Cross, J. B.; Bakken, V.; Adamo, C.; Jaramillo, J.; Gomperts, R.; Stratmann, R. E.; Yazyev, O.; Austin, A. J.; Cammi, R.; Pomelli, C.; Ochterski, J. W.; Ayala, P. Y.; Morokuma, K.; Voth, G. A.; Salvador, P.; Dannenberg, J. J.; Zakrzewski, V. G.; Dapprich, S.; Daniels, A. D.; Strain, M. C.; Farkas, O.; Malick, D. K.; Rabuck, A. D.; Raghavachari, K.; Foresman, J. B.; Ortiz, J. V.; Cui, Q.; Baboul, A. G.; Clifford, S.; Cioslowski, J.; Stefanov, B. B.; Liu, G.; Liashenko, A.; Piskorz, P.; Komaromi, I.; Martin, R. L.; Fox, D. J.; Keith, T.; Al-Laham, M. A.; Peng, C. Y.; Nanayakkara, A.; Challacombe, M.; Gill, P. M. W.; Johnson, B.; Chen, W.; Wong, M. W.; Gonzales, C.; Pople, J. A. *Gaussian 03*, revision D. 01; Gaussian, Inc.: Wallingford, CT, 2004.

(50) Bauernschmitt, R.; Ahlrichs, R. *Chem. Phys. Lett.* **1996**, *256*, 454.

(51) Bauernschmitt, R.; Ahlrichs, R.; Henrich, F. H.; Kappes, M. M. *J. Am. Chem. Soc.* **1998**, *120*, 5052.

(52) Casida, M. E.; Jamorski, C.; Casida, K. C.; Salahub, D. R. *J. Chem. Phys.* **1998**, *108*, 4439.

(53) Hirata, S.; Head-Gordon, M. *Chem. Phys. Lett.* **1999**, *302*, 375.

(54) Salzner, U.; Schleyer, P. v. R. *Chem. Phys. Lett.* **1992**, *199*, 267.

(55) Tour, J. M. *Chem. Rev.* **1996**, *96*, 537.

(56) Rienstra-Kiracofe, J. C.; Tschumper, G. S.; Schaefer, H. F. *Chem. Rev.* **2002**, *102*, 231.

(57) Nakamura, T.; Ando, N.; Matsumoto, Y.; Furuse, S.; Mitsui, M.; Nakajima, A. *Chem. Lett.* **2006**, *35*, 888.

(58) Serrano-Andrés, L.; Merchán, M.; Nebot-Gil, I.; Lindh, R.; Roos, B. O. *J. Chem. Phys.* **1993**, *98*, 3151.

(59) Cossi, M.; Cammi, R.; Tomasi, J. *Chem. Phys. Lett.* **1996**, *255*, 327.

(60) Pariser, R. *J. Chem. Phys.* **1956**, *24*, 250.

(61) Heeger, A. J. Conjugated Polymers: The Interconnection of Chemical and Electronic Structure. In *Conjugated Polymers and Related Materials*; Salaneck, W. R., Lundström, I., Rånby, B., Eds.; Oxford University Press: Oxford, 1993; p 28.

(62) Brédas, J.-L. Electronic Structure of Highly Conducting Polymers. In *Handbook of Conducting Polymers*; Skotheim, T. A., Ed.; Dekker: New York, 1986; p 859.

(63) Boudreaux, D. S.; Chance, R. R.; Brédas, J. L.; Silbey, R. *Phys. Rev. B* **1983**, *28*, 6927.

(64) Villar, H. O.; Dupuis, M.; Clementi, E. *Phys. Rev. B* **1988**, *37*, 2520.

(65) Ehrendorfer, C.; Karpfen, A. *J. Chem. Phys.* **1995**, *99*, 10196.

(66) Brédas, J. L.; Thémans, B.; Fripiat, J. G.; André, J.-M.; Chance, R. R. *Phys. Rev. B* **1984**, *29*, 6761.

(67) Lögdlund, M.; Dannetun, P.; Fredriksson, C.; Salaneck, W. R.; Brédas, J. L. *Synth. Met.* **1994**, *67*, 141.

(68) Irle, S.; Lischka, H. *J. Chem. Phys.* **1995**, *103*, 1508.

(69) Irle, S.; Lischka, H.; Eichkorn, K.; Ahlrichs, R. *Chem. Phys. Lett.* **1996**, *257*, 592.

(70) Lögdlund, M.; Dannetun, P.; Fredriksson, C.; Salaneck, W. R.; Bredas, J. L. *Phys. Rev. B* **1996**, *53*, 16327.

(71) Irle, S.; Lischka, H. *J. Chem. Phys.* **1997**, *107*, 3021.

(72) Salzner, U. *J. Chem. Theor. Comput.* **2007**, *3*, 219.

(73) Zade, S. S.; Bendikov, M. *J. Phys. Chem. B* **2006**, *110*, 15839.

(74) Zade, S. S.; Bendikov, M. *J. Phys. Chem. C* **2007**, *111*, 10662.

(75) Alemán, C.; Julià, L. *J. Phys. Chem.* **1996**, *100*, 14661.

(76) Su, W.-P.; Schrieffer, J. R.; Heeger, A. J. *Phys. Rev. Lett.* **1979**, *42*, 1698.

JP711135E